

# Chemical differentiation of planets: a core issue

Hervé Toulhoat<sup>1</sup>, Valérie Beaumont<sup>1</sup>, Viacheslav Zgonnik<sup>1</sup>, Nikolay Larin<sup>2</sup> and Vladimir N. Larin<sup>3</sup>

<sup>1</sup>IFP Energies nouvelles, 1 & 4 Avenue de Bois Préau, 92852 Reuil-Malmaison Cedex, France

<sup>2</sup>Russian Academy of Science, Schmidt Institute of Physics of the Earth, B.Gruzinskaya St. 10, 123995, Moscow, Russia

<sup>3</sup>Lomonosov Moscow State University, Leninskiye Gory, 119991, Moscow, Russia

## Summary

Prevalent theories of the Solar System formation minimize the role of matter ionization and magnetic field in the Solar nebula. Here we propose that a magnetically driven chemical gradient at the scale of the Solar nebula predates radial chemical differentiation of each planet. We report an observed correlation between the first ionization potentials of the elements and their abundances on Earth surface relative to Sun, interpreted as a Boltzmann distribution depending on the distance from the Sun. This predictive model for distribution of the elements in the Solar System is successfully tested for relative abundance data from CI chondrites, Moon, Mars and Venus. Deviations from the proposed law for a given planet correspond to surface segregation of elements following periodic trends. Bulk Earth would have included up to 18%wt H, with definite consequences on theories about inner Earth composition. From this model, a new picture of the Solar System emerges.

According to the widely accepted model, the Solar System (SS) formed from the gravitational collapse of a fragment of a giant molecular cloud. The accretion of the gas and dust, left over from the Sun's formation, forms planetesimals that collide and aggregate into larger bodies: planets. In this model, the chemical compositions of the planets depend on temperature. In the inner Solar System, which was warm, terrestrial planets form from compounds with high melting points, while more volatile compounds accumulate beyond the so called "ice-line", where they condense to form giant planets. The elemental composition of the most primitive accreting material is supposed to be similar to carbonaceous chondrites of CI group, meteorites that are not chemically fractionated when relative abundances are compared to the photosphere. Hence, the early chemical composition of inner planets is modelled after CI composition. Notwithstanding, inner planets, including Earth, are distinct from any type of extant primitive meteorites or their mixtures<sup>1,2</sup>. Heterogeneous and homogeneous accretion models, together with coherent radial differentiation models integrating geophysical properties of planets, are debated in order to explain observed elemental compositions of planets. Existing accretion and differentiation models are shown to be insufficient to explain the various elemental composition of planetary materials<sup>3</sup>, and more specifically the Earth's<sup>4</sup>. Yet, few decades ago, following space plasma physics-based cosmological theories developed by Hoyle<sup>5</sup>, and by Alfvén and Arrhenius<sup>6</sup> to explain the angular momentum transfer from the Sun to planets, V. Larin<sup>7</sup> proposed that chemical differentiation in the SS was driven by a kind of cyclotronic effect. The gravitational accumulation of the initial interstellar cloud into the protosun determined the formation of a protoplanetary gaseous disk expanding in the plane that was to become the current ecliptic plane. At this stage, this protoplanetary gas was submitted both to ionizing radiations, and a very intense magnetic dipole originating from magneto-hydrodynamics inside the protosun, and that was normal to the disk plane, so that magnetic force lines were also normal to this plane and collinear. A cyclotronic effect ensued whereby orbiting ionized atoms, were attracted towards the protosun by an extra centripetal magnetic Lorentz force

determining a first order spatial distribution of the elements. In support of these views, Larin exhibited a correlation between the log of the abundance of elements on the Earth relative to the Sun, and their first ionization potential (IP). Although, the relationship between IP and chemical composition of Earth and Moon was examined by Hauge<sup>8</sup> with the goal to test Alfvén's<sup>9</sup> theory of the evolution of the SS (which combines electromagnetic forces with gravitational forces), these proposals were not further subjected to theoretical analysis, while other authors report observations<sup>10–13</sup> and theories<sup>14,15</sup> supporting the primary importance of space plasma physical processes in the formation of planetary systems. Herein, a reappraisal of available data for inner SS composition provides opportunity to propose a new predictive model for the distribution of elements in the SS derived from the basic concepts of statistical physics.

### **Magnetically driven chemical differentiation**

The differentiation factor of an element for a planetary body is defined as the ratio of its relative abundance in this body to its relative abundance in the SS with silicon abundances taken as references. Differentiation factors for Earth are computed using Earth crust data<sup>16</sup>, and spectroscopic measured relative abundances in the solar photosphere<sup>16</sup>. The correlation is shown (Fig. 1) for elements from H to U (exclusions and corrections addressed in the supplementary information (SI)). The semi-log plot exhibits an average slope of  $-1.12 \text{ eV}^{-1}$ , with a squared coefficient of correlation of 0.56 (Fig. 1, inset). The physical meaning of this correlation is shown to be linked to electromagnetic forces while observed outliers are linked to radial differentiation as demonstrated hereafter.

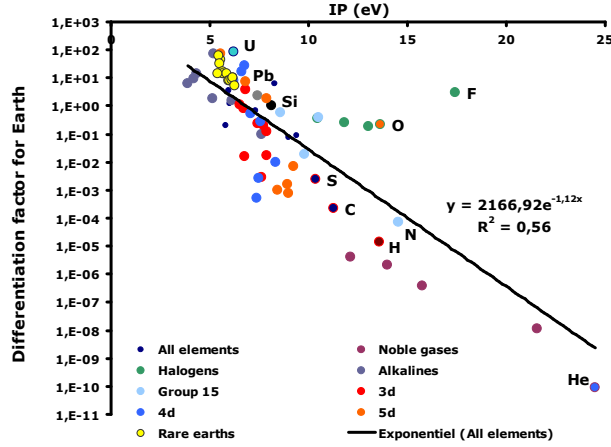


**Figure 1**

Since the abscissa axis in this plot is an energy scale, the law is reminiscent of a Boltzmann distribution. We understand this as follows: beyond their escape distance from gravitational attraction of protosun, atoms in the protoplanetary gaseous disk are flowing away. This determines a net centrifugal flux of matter. However a fraction of this matter becomes ionized, and then is diverted towards equilibrium orbits by the centripetal Lorentz force exerted by the magnetic field normal to the nebular disk. The source of this field would be a strong dipole at the protosun centre. Viewing the ionization potential  $IP(M)$  of a given element  $M$  as the activation energy for its ionization, the molar (or mass) fraction of  $M$   $\left(\frac{X^+}{X_{ss}}(M)\right)$  trapped in orbit at average distance  $d$  from the protosun is proportional to its ionization probability:

$$\left(\frac{X^+}{X_{ss}}(M)\right) = \exp\left(\frac{-IP(M)}{k_B T_{elG}(d)}\right) \quad (1)$$

where  $X_{ss}(M)$  is the initial average abundance of element  $M$  in the SS. Here, we define  $T_{elG}(d)$  as the local electronic temperature of the plasma depending on the distance from the ionizing source. To prescribe this temperature, we assume: 1) that the proto-planetary (very dilute) plasma is

everywhere in equilibrium both with the cosmic background at temperature  $T_{CB}$ , a cool black body, and 2) that the protosun is a black body seen under the solid angle  $\Omega(d)$ . We obtain, as demonstrated in SI:

$$T_{elG} \approx \frac{T_{CB}}{\pi} \left( \frac{d}{R_{PS}} \right)^2 \quad (2)$$

With  $R_{PS}$  the radius of the protosun. According to equation (2), for a dilute atomic cloud irradiated by a black body spectrum of ionizing radiations, electronic thermalization is mainly achieved by ionizing absorption and de-ionizing emission. The ionizing power decreases with the solid angle of sight as distance  $d$  from source increases. Locally, energy is radiated towards the cosmic background preferentially at the expense of the ionized elements with the higher IPs. Therefore, thermal equilibration with cosmic background is obtained by keeping in the ionized state a fraction of the elements, which decreases exponentially as IP increases. At close distance from protosun (e.g.  $d \sim 1$  A.U.), this fraction remains very low even for the lower IPs ( $\sim 4$  eV). As the distance from protosun increases, more elements with higher IPs must be excited in the ionized state. For very large distances, the ratio of ionized over neutral atoms approaches 1, even for the elements with the higher IPs, although the ionizing power of the central body vanishes. Consequently, local electronic temperature increases with the distance to ionizing source.

Finally, considering the normalization of abundances with respect to silicon, and assuming the gravitational aggregation of a planetary body at distance  $d$ , the law of magnetic chemical differentiation of planets comes as:

$$\frac{\left( \frac{X}{X_{Si}} \right)}{\left( \frac{X}{X_{Si}} \right)_{SS}}(d, M) = \exp \left( \frac{-(IP[M] - IP[Si])}{k_B T_{CB}} \pi \left( \frac{R_{PS}}{d} \right)^2 \right) = f_v(M, d) \quad (3)$$

Where  $f_v(M, d)$  is the volumic differentiation factor of a planetary body gravitating at average distance  $d$ , and index  $SS$  refers to the average Solar System. In the case of the Earth ( $d = 1 \text{ A.U.}$ ), using the present times solar radius ( $R_s = 0.009286 \text{ A.U.}$ ) and cosmic background temperature ( $T_{CB} = 2.725 \text{ K}$ ), Eq. (3) predicts a slope  $-1.154 \text{ eV}^{-1}$ , very close to the regression value obtained for elements H to U (Fig. 1,  $-1.12 \text{ eV}^{-1}$ ). Fig. 2 shows the predictions from Eq. (3) for the most inner planets of the SS, and two giant planets (Jupiter and Saturn) on the basis of semi-major axis distances from the Sun. According to our model, beyond asteroid belt, planets elemental composition can not be distinguished from Sun photosphere composition, in consistency with their estimated composition.

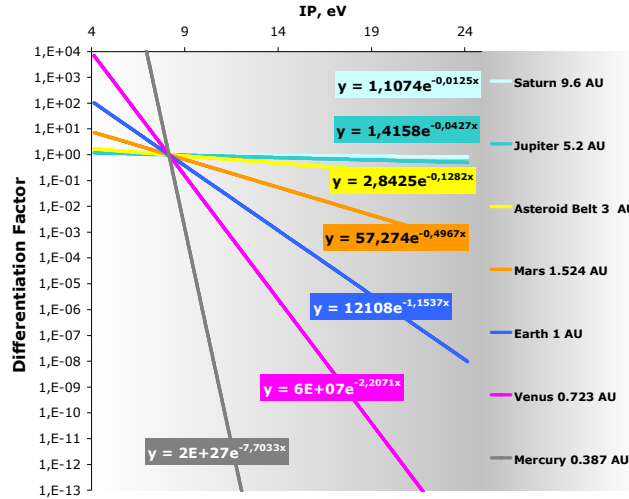


**Figure 2**

Eq. (3) is further tested using chemical analysis data available for asteroid belt and for rocky planetary bodies: Mercury, Venus, Mars and the Moon. Observed differentiation factors versus first ionization potentials are shown in Fig. 3. for asteroid belt (a); Venus (b); Mars (c) and the Moon (d). The slopes of the experimental semi-logarithmic laws (Fig. 3) are compared with theoretical model (Fig. 2).

Considering an average distance to Sun of 3 A.U. for the asteroid belt, Eq. 3 predicts a slope equal to  $-0.13 \text{ eV}^{-1}$ . Using elemental abundances in CI chondritic meteorites<sup>17</sup> supposed to be the main

representatives of asteroid belt<sup>18</sup>, and excluding noble gases and hydrogen, obviously degassed from chondrites, we obtain a striking identity with an experimental slope equal to  $-0.11 \text{ eV}^{-1}$  corresponding to 3.18 A.U. (Fig. 3a) The coefficient of correlation is not very significant, since this slope is quite weak.

Composition of Mercury was taken from the recent data from the MESSENGER mission<sup>19,20</sup>. An experimental slope of  $-0.91$  was obtained against  $-7.6$  expected (Fig. S1 in SI). Large discrepancy from the model can be explained either by nature of data acquisition (small penetrating ability of the MESSENGER X-Ray Spectrometer, analysing exclusively the first micrometers of the surface possibly covered with meteoritic dust), or by Mercury vicinity to the Sun, that makes temperature warmer than  $T_{CB}$  at the time of magnetic differentiation (See SI). In both case one can expect a gentler slope than in Fig. 2, as observed.

Compositions of Venus rock samples from the Venera 13, 14 and Vega 2 missions<sup>21</sup> were completed by the C, Ne,  $^{36}\text{Ar} + ^{38}\text{Ar}$ ,  $^{84}\text{Kr}$  and  $^{129}\text{Xe} + ^{132}\text{Xe}$  from the Venus atmosphere<sup>22</sup>. It renders an experimental slope of  $-1.62$ , against  $-2.20$  expected (Fig. 3b). The experimental slope departure from theory, while an excellent correlation coefficient of 0.91 is obtained, can better be ascribed to a temperature warmer than  $T_{CB}$  in the Venus region during the magnetic differentiation (see SI), the calculated temperature equal to  $T = 3.7 \text{ K}$  is consistent with our model.

Mars composition was calculated after data from the Pathfinder, Opportunity and Spirit missions<sup>23-25</sup>, excluding analysis of soils, which can be affected by meteoritic dust. An experimental slope of  $-0.46$  is observed for  $-0.49$  expected (because high IP element abundances are not available, especially those of noble gases, three outliers, P, Cl and Br, which were segregated onto the surface during subsequent radial differentiation, (explanations hereafter and in SI) are truncated). Beyond Venus, for Mars as well as for the Earth and asteroid belt, elemental abundances are thus dependant on the distance to the Sun, no temperature effect is observed.

Fig. 3d was built after experimental data from missions Apollo 15, 16 and 17 <sup>(ref. 26)</sup> to the Moon. For each element the mass fraction is averaged after all stations for all missions. Excluding O and F, an experimental slope of -1.21 is observed against -1.12 observed for the Earth (Fig. 1). The result is consistent with Moon elements inherited in close vicinity of the Earth (See details in SI) in agreement with other models<sup>27</sup>.

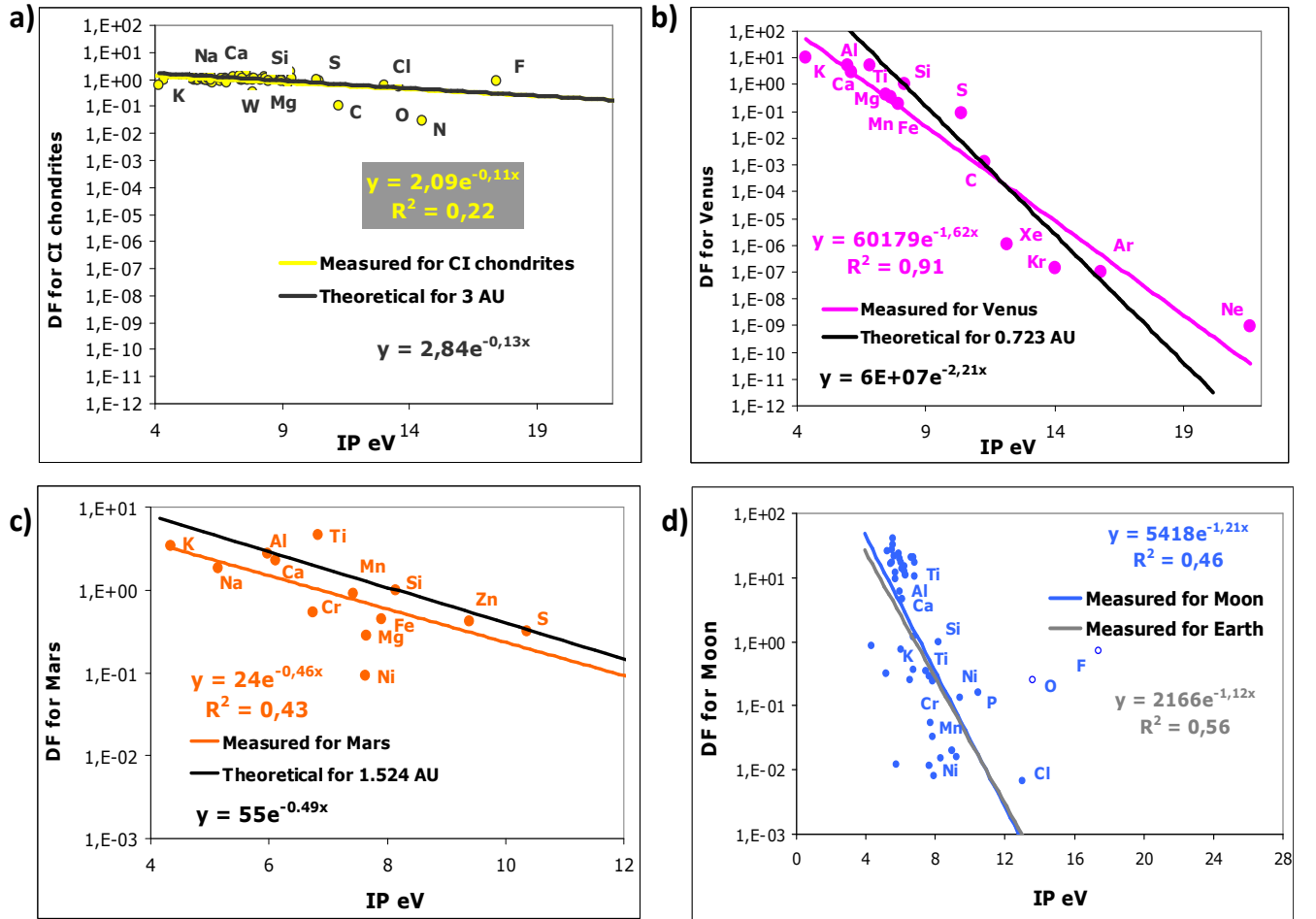


Figure 3

### Radial differentiation inside Earth: chemistry versus gravity

In Fig. 1, differentiation factors of the elements are calculated after experimental elemental abundances measured and averaged for the crust, hydrosphere and atmosphere, i.e. Earth surface, while

Eq. 3 should hold for the relative abundances averaged over the bulk Earth volumic relative abundances  $f_{EV}(M)$ . Accordingly, departures from law described by Eq. 3 (vertical distances in Log scale to the regression line) straightforwardly convey the information on the ratio of surface to volume concentrations. This is expressed by Eq. 4 demonstrated in SI:

$$\text{Ln}\left(\frac{X_{ES}}{X_{EV}}(M)\right) = [\text{Ln}f_{ES}(M) - \text{Ln}f_{EV}(M)] + \text{Ln}\left[\sum_M X_{ES}(M) \frac{f_{EV}(M)}{f_{ES}(M)}\right] \quad (4)$$

where indices  $ES$  and  $EV$  stand for Earth surface and Earth volume respectively. Hence, crust data points located above the regression line stand for elements which are enriched at the surface relative to volume (e.g. F, O, Si, P, B, Cl...), or added from outer space to surface; whereas those located below stand for elements which are depleted in surface, relative to volume (e.g. Fe, Co, Ni, Cr, H, ...) or lost through escape to space (notably H, He).

Plotting those partition coefficients,  $\text{Ln}\left(\frac{X_{ES}}{X_{EV}}(M)\right)$  against atomic mass (Fig. 4), reveals

distinctive periodic trends in the depletion or enrichment in chemical elements at the Earth surface with respect to Earth volume:

- Noble gases are increasingly depleted from the surface with increasing atomic mass, in an approximately linear trend (exclusions and corrections: see in SI). Since noble gases can be considered as chemically inert, this trend is interpreted as purely gravity driven (buoyancy) radial differentiation.
- Rare earth elements are systematically more abundant at the surface, with similar partition coefficients.
- The most electronegative elements, O and halogens, are much more abundant at the surface than in volume. Halogens are the sole elements with positive heats of formation of their oxides, while it is zero by convention for  $\text{O}_2(\text{g})$  itself.

- Transition elements in the 3d, 4d and 5d series exhibit complex periodic patterns, with the elements from groups 3 to 5 enriched at the surface, then increasing depletion in favor of volume with d-band filling, going through a maximum for Ni, Ru and Os, then decreasing again.

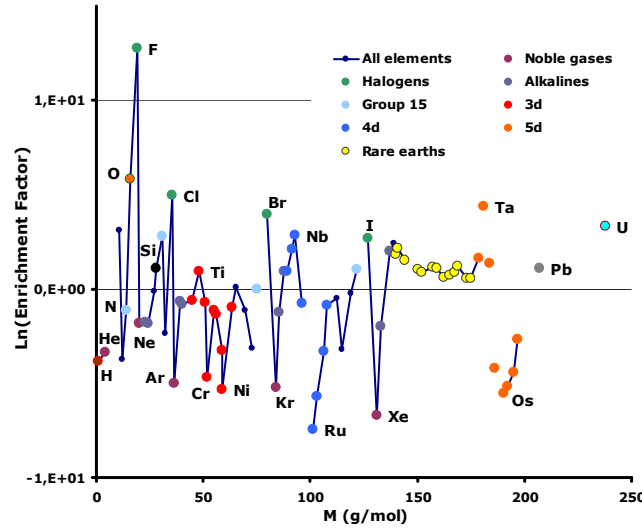


Figure 4

## Discussion

According to Eqs. 3 and 4, considering as traces the elements heavier than Ni, and making use of available experimental relative abundances for Earth crust, initial bulk mass fractions for Earth  $X_{EV}(M)$  can be calculated (Table S1, first column, in SI). This calculation predicts a very high initial content of H in inner Earth, second major element after Fe, and a surprisingly low content of O:

$$\text{Fe} > \text{H} > \text{Mg} > \text{Na} > \text{Si} > \text{Ca} > \text{Al} > \text{K} > \text{Ni} > \text{Cr} > \text{C} > \text{S} > \text{Ti} > \text{O}$$

The ranking of mole fractions (Table S1, second column, in SI) reflects the bulk abundances in terms of atomic populations and allow stoichiometric guesses:

$$\text{H} \gg \text{Na} > \text{Mg} > \text{Fe} > \text{Al} > \text{Si} > \text{Ca} > \text{K} > \text{C} > \text{Cr} > \text{S} > \text{Mn} \sim \text{O} > \text{Ti}$$

The bulk mass and mole fractions we deduce reveal that the early Earth has been more H-rich and O-poor than currently considered. In quantitative terms Eq. 4 yields up to an initial hydrogen content of 18.3 wt % for the early Earth. The low escape speed for molecular hydrogen at Earth surface favours its diffusion towards outer space in the absence of oxidizing agents in the atmosphere (as suggested for early Earth) however chemically and physically bonded H could not escape. Since the accepted stoichiometries for hydrides of the major and minor elements according to the obtained elemental bulk composition would immobilize only about 23 mole % of the amount of H initially available, inner Earth may have contained  $9 \cdot 10^{11}$  Gt (4.7 wt % of the Earth) of hydrogen. Yet, iron hydride is considered as a key ingredient of Earth's core<sup>28,29</sup> to resolve the so-called "core density deficit problem". The present results suggest that Earth's mantle can potentially be more reducing than usually considered and hydrogen is more evenly distributed in the SS than previously thought.

The proposed model provides an opportunity to address in a new light unresolved issues: the transfer of angular momentum, the origin of volatiles, the initial composition of planets in the Solar system, the driving forces for radial differentiation... It opens the way to estimation of chemical composition of exoplanets. It predicts that the Earth elemental composition is drastically different from current estimation with many consequences beyond the scope of this paper, notably potential future supply of clean primary energy. Exploring its potential is therefore a core issue.

## References

1. Campbell, I.H. & St C. O'Neill, H. Evidence against a chondritic Earth. *Nature* **483**, 553-558 (2012).
2. Drake, M.J. & Richter, K. Determining the composition of the Earth. *Nature* **416**, 39-44 (2002).
3. Bertka, C.M. Implications of Mars Pathfinder Data for the Accretion History of the Terrestrial Planets. *Science* **281**, 1838-1840 (1998).
4. Javoy, M. Chemical Earth models. *C. R. Académie des Sciences Paris* **329**, 537-555 (1999).
5. Hoyle, F. On the origin of the solar nebula. *Quarterly Journal of the Royal Astronomical Society* **1**, 28-55 (1960).
6. Alfvén, H. & Arrhenius, G. *Evolution of the solar system*. 599 p., (Scientific and Technical Information Office, National Aeronautics and Space Administration: Washington, 1976).
7. Larin, V.N. *Hydridic Earth: the New Geology of Our Primordially Hydrogen-rich Planet*. 256 p., (Polar publishing: Alberta, 1993).
8. Hauge, Ö. Observed Abundance Distribution of Chemical Elements as a Test of Alfvén's Theory of the Origin of the Solar System. *Nature* **230**, 39-41 (1971).
9. Alfvén, H. *On the origin of the solar system*. 194 p., (Clarendon Press: Oxford, 1954).
10. Lundin, R. & Marklund, G. Plasma vortex structures and the evolution of the solar system—the legacy of Hannes Alfvén. *Physica Scripta* **T60**, 198-205 (1995).
11. Donati, J.-F., Paletou, F., Bouvier, J. & Ferreira, J. Direct detection of a magnetic field in the innermost regions of an accretion disk. *Nature* **438**, 466-9 (2005).
12. Bonnevier, B. Experimental evidence of element and isotope separation in a rotating plasma. *Plasma Physics* **13**, 763-774 (1971).
13. Geiss, J. Constraints on the FIP mechanisms from solar wind abundance data. *Space science reviews* **85**, 241-252 (1998).
14. Eneev, T.M. & Kozlov, N.N. A model of the accumulation process in the formation of planetary systems. I. Numerical experiments. *Solar System Research* **15**, 59-70 (1981).
15. Eneev, T.M. & Kozlov, N.N. A model of the accumulation process in the formation of planetary systems. II. Rotation of the planets and the relation of the model to the theory of gravitational instability. *Solar System Research* **15**, 97-104 (1982).
16. *CRC Handbook of Chemistry and Physics 73rd Edition*. (CRC Press: Boca Raton, 1992).
17. Lodders, K. Solar system abundances and condensation temperatures of the elements. *The Astrophysical Journal* **591**, 1220-1247 (2003).

18. Scott, E.R.D. & Krot, A.N. Chondrites and Their Components. *Treatise on Geochemistry* **1.07**, 1-72 (2007). doi:10.1016/B0-08-043751-6/01145-2
19. Nittler, L.R. *et al.* The Major-Element Composition of Mercury's Surface from MESSENGER X-ray Spectrometry. *Science* **333**, 1847-1850 (2011).
20. Peplowski, P.N. *et al.* Radioactive Elements on Mercury's Surface from MESSENGER: Implications for the Planet's Formation and Evolution. *Science* **333**, 1850-1852 (2011).
21. Abdrakhimov, A.M. & Basilevsky, A.T. Geology of the Venera and Vega Landing-Site Regions. *Solar System Research* **36**, 136-159 (2002).
22. Fegley, B.J. Venus. *Treatise on Geochemistry* **1.19**, 487-507 (2007). doi:10.1016/B0-08-043751-6/01150-6
23. Foley, C.N. Final chemical results from the Mars Pathfinder alpha proton X-ray spectrometer. *Journal of Geophysical Research* **108**, (2003).
24. Hahn, B. The Chemical Composition and Evolution of the Martian Upper Crust and Near Surface Environment. 162 p., (2009).
25. Arvidson, R.E. *et al.* Spirit Mars Rover Mission: Overview and selected results from the northern Home Plate Winter Haven to the side of Scamander crater. *Journal of Geophysical Research* **115**, (2010).
26. Wanke, H. *et al.* Multielement analyses of Apollo 15, 16, and 17 samples and the bulk composition of the moon. *Lunar and Planetary Science Conference Proceedings* **4**, 1461-1481 (1973).
27. Ringwood, A.E. Terrestrial origin of the Moon. *Nature* **322**, 323-328 (1986).
28. Isaev, E.I., Skorodumova, N.V., Ahuja, R., Vekilov, Y.K. & Johansson, B. Dynamical stability of Fe-H in the Earth's mantle and core regions. *Proceedings of the National Academy of Sciences of the United States of America* **104**, 9168-71 (2007).
29. Badding, J.V., Hemley, R.J. & Mao, H.K. High-pressure chemistry of hydrogen in metals: in situ study of iron hydride. *Science* **253**, 421-424 (1991).

## Author contributions

H.T. planned the research on the basis of the early semi-quantitative ideas from V.L., developed the equations, performed the tests against experimental data and wrote the first drafts; V.Z. assured the collaboration between French and Russian teams; V.B., V.Z. and N.L. gathered literature data and contributed to numerical tests; all authors contributed to criticize and improve the interpretation and to write the final form of the manuscript.

## Author information

Reprints and permissions information is available at [www.nature.com/reprints](http://www.nature.com/reprints). The authors declare no competing financial interests. Correspondence and requests for materials should be addressed to H.T. ([herve.toulhoat@ifpen.fr](mailto:herve.toulhoat@ifpen.fr), tel. +33 147527350).

## Figure legends

**Figure 1:** Earth crust differentiation factors vs first ionization potential for elements H to U. The slope of the regression line in the semi-log plot, excluding He is  $-1.12 \text{ eV}^{-1}$ .

**Figure 2:** Correlation existing between differentiation factors for bulk planets and first ionization potential, according to Eq. (3) with T equal to the T of cosmic background: obviously terrestrial planets only will exhibit noticeable differences from photosphere (for the photosphere  $y = 1$ ).

**Figure 3:** Differentiation factors (DF) versus first ionization potentials for: **a)** CI chondrites, **b)** Venus, **c)** Mars, **d)** Moon. Explanations are inside the text. Outliers: empty symbols.

**Figure 4:** Earth surface to volume partition coefficients versus atomic weights for elements H to U.

## Supplementary Information

### Supplementary Methods

#### Calculation of the differentiation factor for Earth

In addition to average crust, the relative abundances were corrected using data from hydrosphere and atmosphere<sup>1</sup>. A special attention is given to radiogenic nuclides. Helium is not considered in calculations as, in addition to primordial  $^3\text{He}$  and  $^4\text{He}$ ,  $^3\text{He}$  is produced from  $^6\text{Li}$  while  $^4\text{He}$  is produced during decay of different radionuclides. In these conditions significant differentiation factors can not be calculated for He. Earth value for Argon abundance excludes  $^{40}\text{Ar}$  that is essentially radiogenic, and produced from  $^{40}\text{K}$ , with Ar and K displaying very different IP's (15.75 and 4.34 eV, respectively). Xe abundances are not corrected from radiogenic  $^{129}\text{Xe}$  produced from  $^{129}\text{I}$ , since Xe and I display similar IP's (12.13 and 10.45 eV respectively). The contribution of radiogenic  $^{21}\text{Ne}$  is considered as negligible and therefore Ne abundances were not corrected. Li and Be that are burnt during nucleosynthetic reactions in the Sun are not reported (B might have been also affected).

It should be noted, that when analysis is restricted to major elements onto the surface, results doesn't fit the predicted curve, because the surface composition is affected by radial differentiation processes.

#### Supplementary Equations

##### Demonstration of Eq. 3:

We consider the protoplanetary gas as a dilute atomic plasma, absorbing radiation from the protosun and emitting towards the cosmic background. Locally (at distance  $d$  from the protosun) and at the microscopic space and time scale, the absorption (or emission) spectrum will exhibit strong lines corresponding to the electronic transitions for ionizations. Therefore it cannot be described by the Planck's law of blackbody radiation, in particular in the range of energy  $\sim 4\text{-}25$  eV corresponding to photons able to trigger the first ionization of the chemical elements.

In that range of energy the power absorbed per unit volume of gas is therefore strictly proportional to the flux of photons from the protosun, itself proportional to  $\Omega(d)$  the local solid angle of observation of the proto-sun:

$$\Omega(d) = \pi \left( \frac{R_{PS}}{d} \right)^2 \quad (S1)$$

Introducing the local electronic temperature of the protoplanetary gas  $T_{elG}(d)$  defined by Eq. 1 allows to express the ionization probability for element M:

$$\left( \frac{X^+}{X_{ss}}(M) \right) = \exp \left( \frac{-IP(M)}{k_B T_{elG}(d)} \right) \quad (1)$$

Once a stationary regime has been reached, the average local kinetic energy of the gas is locally equal to the average local input of radiative energy so that:

$$k_B T_G(d) = k_B T_{elG}(d) \pi \left( \frac{R_{PS}}{d} \right)^2 \quad (S2)$$

with  $T_G(d)$  the local protoplanetary gas temperature.

On the other hand, macroscopically, that is at the astronomical space and time scales, the protoplanetary plasma can be considered as a thermalized blackbody in equilibrium with the Cosmic Background, so that for any distance  $d$  far enough from protosun:

$$T_G(d) \approx T_{CB} \quad (S3)$$

where  $T_{CB}$  is the Cosmic Background temperature, and therefore:

$$k_B T_{CB} = k_B T_{elG}(d) \pi \left( \frac{R_{PS}}{d} \right)^2 \quad (S4)$$

$$\left( \frac{X^+}{X_{SS}}(M) \right) = \exp \left( \frac{-IP(M)}{k_B T_{CB}} \pi \left( \frac{R_{PS}}{d} \right)^2 \right) \quad (S5)$$

Substituting for  $T_{elG}(d)$  in (1), yields Eq. (S5), related to Eq. 3:

Besides, if the protoplanetary gas precursor to planets closer to the Sun than Earth was hotter than  $T_{CB}$ , it will result in a corrected exponent  $\frac{T_{CB}}{T} \left( \frac{1}{d} \right)^2$ . This may happen for Mercury (Fig. S1), and for Venus (Fig. 3b).

#### **Demonstration of Eq. 4:**

The demonstration is straightforward, noticing that for all elements  $M$  :

$$\frac{X_{ES}}{X_{EV}}(M) = \frac{\left(\frac{X_{ES}(M)}{X_{ES}(Si)}\right) \left(\frac{X_{SS}(M)}{X_{SS}(Si)}\right) X_{ES}(Si)}{\left(\frac{X_{EV}(M)}{X_{EV}(Si)}\right) \left(\frac{X_{SS}(M)}{X_{SS}(Si)}\right) X_{EV}(Si)} \quad (S11)$$

with indices  $ES$ ,  $EV$ ,  $SS$ , for Earth Surface, Earth Volume and average Solar System respectively. By definition of the differentiation (or enrichment) factors  $f_i(M)$  (see main text), it follows:

$$\frac{X_{ES}}{X_{EV}}(M) = \frac{f_{ES}(M)}{f_{EV}(M)} \frac{X_{ES}}{X_{EV}}(Si) \quad (S12)$$

The overall mass balance for Earth requires:

$$\sum_M X_{EV}(M) = 1 \quad (S13)$$

or, using (S2):

$$\sum_M X_{ES}(M) \frac{f_{EV}(M)}{f_{ES}(M)} = \frac{X_{ES}(Si)}{X_{EV}(Si)} \quad (S14)$$

from which one determines:

$$X_{EV}(Si) = \frac{X_{ES}(Si)}{\sum_M X_{ES}(M) \frac{f_{EV}(M)}{f_{ES}(M)}} \quad (S15)$$

or:

$$X_{EV}(Si) = \frac{1}{1 + \sum_{M \neq Si} f_{EV}(M) \left( \frac{X_{SS}(M)}{X_{SS}(Si)} \right)} \quad (S16)$$

Since  $f_{EV}(M)$  is known for all elements from Eq. 3, and all relative abundances in the solar system are known from experiment, equations (S12) and (S16) allow to determine all average mass fractions for the whole Earth volume, including that of element  $H$ .

Combining (S12) and (S15):

$$\frac{X_{ES}}{X_{EV}}(M) = \frac{f_{ES}(M)}{f_{EV}(M)} \sum_M X_{ES}(M) \frac{f_{EV}(M)}{f_{ES}(M)} \quad (S17)$$

Taking the natural logarithm of both sides of Eq. (S17), one gets Eq. 4:

$$\ln \left( \frac{X_{ES}}{X_{EV}}(M) \right) = [\ln f_{ES}(M) - \ln f_{EV}(M)] + \ln \left[ \sum_M X_{ES}(M) \frac{f_{EV}(M)}{f_{ES}(M)} \right] \quad (4)$$

## Supplementary Discussion

### Differentiation factor for Mercury

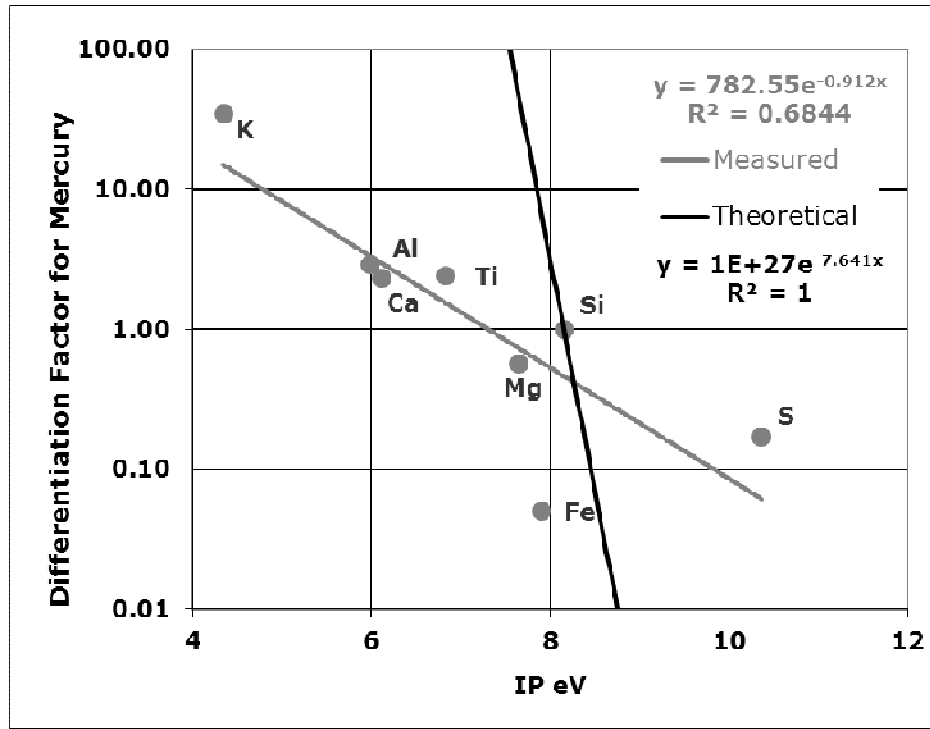


**Figure S1:** Differentiation factors versus first ionization potentials  $IP$  for Mercury.

Higher experimental slope obtained for Mercury and Venus can be attributed to a temperature effect in the close vicinity of the Sun. Accordingly, we calculate a temperature of  $T=22.8$  K for Mercury vicinity and  $T= 3.7$  K for Venus vicinity at the time of radial differentiation.

Notice that the high abundance of K (low IP), determined by the MESSENGER Gamma-Ray Spectrometer<sup>2</sup>, is in agreement with our model, while in an elemental distribution model dependant on the temperatures of condensation this element would not be enriched on Mercury.

### Differentiation factors for Mars and Moon

For Mars and Moon, we also plot averaged differentiation factors of major elements computed from in-situ analyses of rock samples versus data for Earth crust. From Eq. 3 we expect power law

relationships with exponents  $\left(\frac{1}{d}\right)^2$  where  $d$  in A.U. stands for the considered planet's distance to the Sun. This method enables comparison of the available elements, in absence of elements with high IPs, and smooths the effects of radial differentiation (the same elements being globally subjected to the same effects regardless of the planet). Figures S2 and S3 represent differentiation factors for Mars *vs.* Earth and Moon *vs.* Earth, respectively.

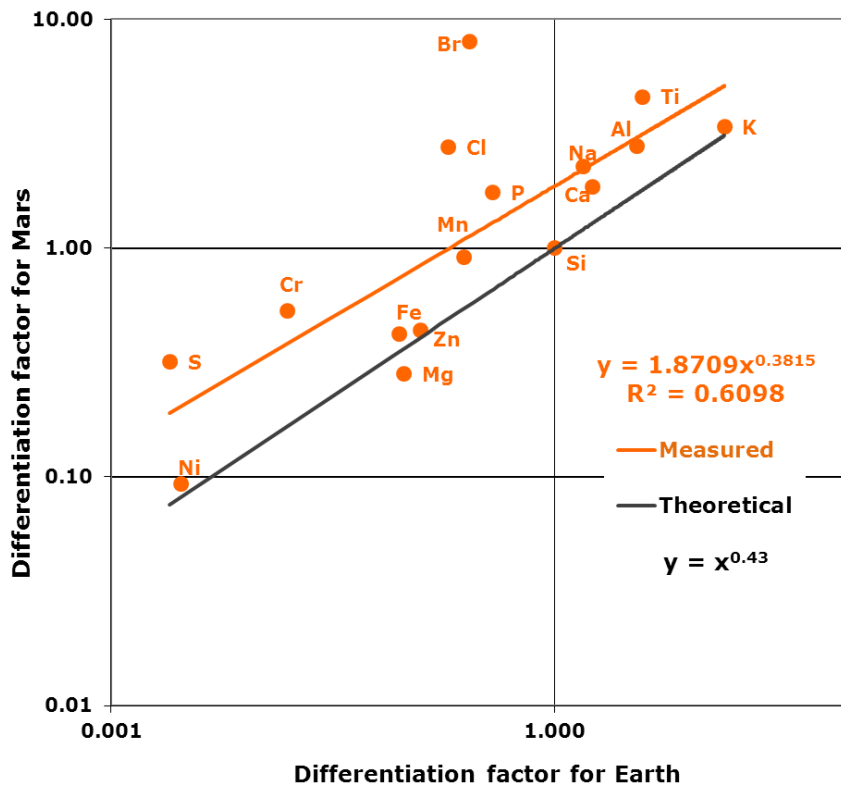


**Figure S2:** Averaged differentiation factors for Mars versus data for Earth crust.

The obtained slope of 0.38 correspond to a distance from Mars to Sun equal to 1.62 AU which compared very well to present distance of 1.66 AU for aphelion and 1.38 AU for perihelion.

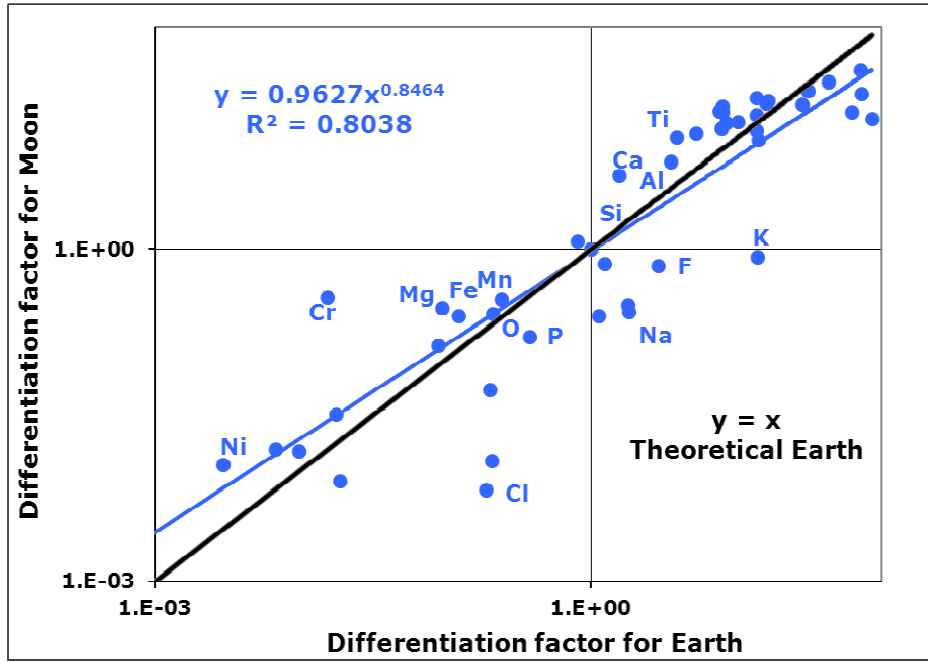


**Figure S3:** Averaged differentiation factors for Moon versus data for Earth crust.

The least square regression law gives a squared coefficient of correlation 0.8, and according to Eq. 3, the exponent 0.85 corresponds to

$$d_{Moon} = \frac{1}{\sqrt{0.85}} = 1.084 \text{ A.U.}$$

The first bissector in the Log-Log plot corresponds to

$$d_{Moon} = \frac{1}{\sqrt{1}} = 1 \text{ A.U.}$$

The result, a distance  $d = 1.084 \text{ A.U.}$  (least square regression line) that can not be distinguished from  $d = 1 \text{ A.U.}$  due to uncertainties.



## Supplementary Table

### Predicted initial bulk composition of the Earth

Element	wt %	mol %
<b>H</b>	<b>1.830E+01</b>	<b>87.43</b>
He	1.856E-05	<0.01
B	4.220E-05	<0.01
<b>C</b>	<b>7.550E-01</b>	<b>0.30</b>
N	5.562E-03	<0.01
<b>O</b>	<b>1.391E-01</b>	<b>0.04</b>
F	1.260E-07	<0.01
Ne	2.675E-06	<0.01
<b>Na</b>	<b>1.341E+01</b>	<b>2.81</b>
<b>Mg</b>	<b>1.389E+01</b>	<b>2.75</b>
<b>Al</b>	<b>8.769E+00</b>	<b>1.57</b>
<b>Si</b>	<b>9.028E+00</b>	<b>1.55</b>
P	5.715E-03	<0.01
<b>S</b>	<b>3.793E-01</b>	<b>0.06</b>
Cl	4.210E-04	<0.01
Ar	1.883E-04	<0.01
<b>K</b>	<b>3.760E+00</b>	<b>0.46</b>
<b>Ca</b>	<b>8.792E+00</b>	<b>1.06</b>
Sc	3.601E-03	<0.01
<b>Ti</b>	<b>2.100E-01</b>	<b>0.02</b>
V	2.329E-02	<0.01
<b>Cr</b>	<b>1.046E+00</b>	<b>0.10</b>
<b>Mn</b>	<b>4.518E-01</b>	<b>0.04</b>
<b>Fe</b>	<b>1.942E+01</b>	<b>1.67</b>
Co	6.153E-02	0.01
<b>Ni</b>	<b>1.627E+00</b>	<b>0.13</b>
Balance	1,00E+02	100

**Table S1:** Predicted overall initial composition of the Earth. Major elements are typed in bold (mass fraction larger than 0.1%). Values for major and minor elements ( >10<sup>-4</sup> g.g<sup>-1</sup> or >10<sup>-2</sup> mol% ) are typed in bold.

## References

1. *CRC Handbook of Chemistry and Physics 73rd Edition*. (CRC Press: Boca Raton, 1992).
2. Peplowski, P.N. *et al.* Radioactive Elements on Mercury's Surface from MESSENGER: Implications for the Planet's Formation and Evolution. *Science* **333**, 1850-1852 (2011).